



Published in final edited form as:

J Med Chem. 2010 June 24; 53(12): 4623–4632. doi:10.1021/jm100092s.

Identification and Functional Characterization of a Stable, Centrally Active Derivative of the Neurotensin (8–13) Fragment as a Potential First-in-Class Analgesic

Francis M. Hughes Jr.^{1,2}, Brooke E. Shaner¹, Lisa A. May¹, Lyndsay Zotian¹, Justin O. Brower², R. Jeremy Woods², Michael Cash², Dustin Morrow¹, Fabienne Massa³, Jean Mazella³, and Thomas A. Dix^{1,2,*}

¹Department of Pharmaceutical and Biomedical Sciences, South Carolina College of Pharmacy, Medical University of South Carolina Campus, 280 Calhoun Street, P. O. Box 250140, Charleston, SC 29425-2303, USA

²Argolyn Bioscience, Inc. 2530 Meridian Parkway, Suite 200, Durham, NC 27713, USA

³Institut de Pharmacologie Moléculaire and Cellulaire, UMR 6097, Université de Nice-Sophia Antipolis, Centre National de la Recherche Scientifique, 660 route des Lucioles, 06560, Valbonne, France

Abstract

The neurotensin hexapeptide fragment NT(8–13) is a potent analgesic when administered directly to the central nervous system, but does not cross the blood brain barrier. A total of 43 novel derivatives of NT(8–13) were evaluated with one, ABS212 (**1**), being most active in four rat models of pain when administered peripherally. Compound **1** binds to human neurotensin receptors 1 and 2 with IC₅₀s of 10.6 and 54.2 nM, respectively and tolerance to the compound in a rat pain model did not develop after 12 days of daily administration. When administered peripherally, serum levels and neurotensin receptor binding potency of **1** peaked within 5 min and returned to baseline within 90–120 min, however analgesic activity remained near maximum for >240 min. This could be due to its metabolism into an active fragment; however, all 4- and 5-mer hydrolysis products were inactive. This pharmacokinetic/pharmacodynamic dichotomy is discussed. Compound **1** is a candidate for development as a first-in-class analgesic.

Introduction

Neurotensin (NT) is a tridecapeptide first isolated from bovine hypothalamus over 30 years ago ¹. The hexapeptide C-terminal fragment NT(8–13) [Arg⁽⁸⁾-Arg⁽⁹⁾-Pro⁽¹⁰⁾-Tyr⁽¹¹⁾-Ile⁽¹²⁾-Leu⁽¹³⁾] was shown to retain the full activity of the parental compound **2**, defining it as the active component of the molecule and the logical lead for development of NT-based therapeutics. Although its effects are not limited to the nervous system ^{3–4}, NT is known to act as a neurotransmitter/neuromodulator where it induces several important physiological effects in mammals including analgesia ⁵ and hypothermia ⁶. It also has been shown to have potential as an antipsychotic compound based on its blockade of amphetamine-induced locomotor hyperactivity ^{7–8}. NT exerts its effects through binding of two brain receptors, NTR-1 (also referred to as NTS-1) and NTR-2 (NTS-2), although the relative roles of each receptor in the physiological responses are not well-understood ^{9–11}. Numerous experiments with both NT and NT(8–13) suggest that all central activities attributable to NT

*To whom correspondence should be addressed. Address: Department of Pharmaceutical and Biomedical Sciences, Medical University of South Carolina, 280 Calhoun St. QF304, Charleston, SC 29403, Tel: 843-876-5092, dixta@musc.edu.

and derivatives only manifest following direct application into the CNS¹² while peripheral administration is ineffectual. This probably is a result of the compounds' polarity and short half-lives in plasma¹³. Hence, NT derivatives that could be delivered peripherally and cross the BBB would have great potential for development as pharmaceutical agents.

Two previously described NT(8–13) analogs (NT1 and NT69L) displayed significant analgesic and antipsychotic effects when injected i.p.^{14–15}. However, various aspects limited their usefulness as a drug including the induction of significant tolerance after a single injection¹⁶. Research in this laboratory and others have shown that minor changes to the structure of NT(8–13) can effect extreme changes in hypothermic, antipsychotic or analgesic responses^{12–13,15,17–19}. Specifically, modification of the N-terminus of NT(8–13) and substitution of *t*Leu at position 12 produce compounds exhibiting increased stability in blood and antipsychotic activity in rats^{19–20} (also unpublished data); the most active of these compounds is ABS201 (**2**)²¹ (Compound **11** in earlier manuscript).

Compound **2** also exhibits minor analgesic activity. In this paper, structural modification of **2** and subsequent evaluation in various rat models have been used to identify new NT(8–13) derivatives possessing dramatically improved analgesic properties. A library of 44 proprietary modifications to the NT(8–13) parent compound have been screened, with ABS212 (**1**) chosen as the lead compound based on its superior activity in the hot plate model. Compound **1** was further screened in a battery of analgesic models, and its pharmaceutical properties explored, in order to evaluate its potential for further development as a first-in-class analgesic.

Results

Synthesis of analogs

NT and NT(8–13) are pluripotent peptides that have activity as analgesics, antipsychotic and hypothermic agents, only when administered directly into the CNS. Previously, we developed a derivative of NT(8–13), **2**, that has potent antipsychotic but weak analgesic properties when dosed i.p. or i.v.¹³. This analog possesses several significant alterations from the parental compound including a modified N-terminus and Arg⁸ residue, and substitution of *t*Leu for Ile¹². The primary result of these alterations was to block peptidase-catalyzed hydrolysis at Arg⁸-Arg⁹ and Tyr¹¹-Ile¹², respectively²². To expand upon previous findings, a series of 43 additional analogs were synthesized that feature further modification of the N-terminus and Arg residue with the anticipation that we would uncover compounds featuring changes/improvements in their relative antipsychotic/analgesic profiles. The structures of the new peptides are given in Figure 1.

Analysis of analogs in the hotplate model

As an initial screen for analgesic activity, all peptides were evaluated in the hotplate analgesic model using a standard dosing of 10 mg/kg i.p. This value was an approximate molar equivalent dose to 5 mg/kg morphine to provide a potency benchmark. Figure 2 shows a typical pharmacodynamic (PD) response curve comparing **1** to morphine and saline. For morphine the response reaches 100% of the maximal possible effect (MPE) after 15–30 min and then decreases in a time-dependent manner, returning to baseline by 200 min. When dosed with **1**, the time at 100% MPE was greatly prolonged and did not begin to diminish significantly for 180 min. The remaining compounds in Figure 1 also were tested in this model.

In order to facilitate a meaningful comparison of relative potency of all compounds tested, Table 1 reports three major endpoints of the model; 1) the maximal effect (as a percentage of the MPE) obtained with the given compound, 2) the time that 100% MPE was maintained

and 3) the area underneath the PD response curve. Analysis of that table indicates that **1** was the most efficacious of the analogs and thus was chosen for further study.

Potency of **1** with various routes of administration

Potency studies were undertaken to determine the EC₅₀ of **1** and to evaluate whether it differed as a function of the route of administration. As shown in Figure 3, the EC₅₀ of **1** was 2.64 mg/kg when delivered i.v. Significant differences were not found when the drug was administered i.p., s.c. or i.m.

Effect of **1** in other models of pain

To evaluate the potential usefulness of **1** as a general analgesic, its effectiveness in four additional rat models of pain (acetic acid writhing, tail flick, formalin and Chung models) was determined. As shown in Figure 4, **1** was quite potent in the acetic acid writhing assay with an EC₅₀ of 0.16 mg/kg (approximately 10-fold more potent than the hot plate). This increase in potency relative to the hot plate may be a result of the high sensitivity of this assay 23–24. In the tail flick assay (Figure 5A), **1** significantly increased the latency of tail withdrawal (indicated at the %MPE) in a manner similar to morphine. A dose response analysis revealed an EC₅₀ of 1.84 mg/kg, very similar to what was seen in the hotplate assay (Figure 5B). Figure 6A presents a typical PD response curve in the formalin model. Compound **1** again was significantly more potent than morphine in this model. The dose response curve (Figure 6B) indicated an EC₅₀ of 2.05 mg/kg, again similar to the hotplate model. In the Chung model of neuropathic pain (Figure 7; performed at a single dose of 10 mg/kg) **1** elicits a maximal response within 15 min which is maintained for over one hour before beginning to fade.

Effect of **1** on hypothermia

A well-known central effect of NT and its active derivatives is the reduction of core body temperature (hypothermia). Figure 8A is a typical PD response curve obtained with **1** that demonstrates a significant and sustained (>4 h) drop in temperature. Interestingly, the dose response curve of the area under the PD curves (Figure 8B) gave an EC₅₀ of 0.78 mg/kg, significantly lower than the EC₅₀s associated with central pain mediation. This is likely due to the hypothermic and analgesic effects being modified through different NTRs.

Lack of induction of tolerance by **1**

Previously reported NT analogs have been shown to induce tolerance after as little as a single injection 16. In order to assess potential development of tolerance to **1**, rats were injected with 10 mg/kg daily for 12 consecutive days. On the indicated days (Figure 9) rats were analyzed in the hotplate analgesia model immediately following injections. As seen in Figure 2, initial injections resulted in a strong and sustained increase in response latency in this assay, again demonstrating the significant analgesic activity of this compound. However, even after 12 daily injections, the animals still displayed a similar PD response, clearly showing that tolerance is not developing to **1** over the time course of the experiments.

Binding to NTRs

To insure that **1** is binding to appropriate receptors with sufficient affinity to effectuate the PD responses, binding assays were performed with rat NTR-1. As shown in Figure 10A there was dose-dependent binding of **1** to rat NTR-1 with a K_D of 23.31 nM. Equivalent experiments could not be performed with cloned rat NTR-2 as various investigators have not been able to obtain stable constructs (E. Richelson, personal communication). However, the binding to human NTR-1 and NTR-2 was assessed and demonstrated EC₅₀s of 10.6 nM and

54.2 nM, respectively. For virtually all NT derivatives, their relative affinities for human versus rat NTRs remain consistent 25–26.

Calcium mobilization

To insure that binding to receptor actually results in activation, the flux of calcium (a well established second messenger response) was measured in the rat NTR-1 expressing cells in response to increasing concentrations of **1**. As shown in Figure 10B **1** activated calcium flux with an EC₅₀ of 27.9 nM, a concentration very similar to its binding affinity.

PK Analysis

As a further step towards understanding the mechanism of action of **1**, a PK analysis was performed. After injection of rats with 1 mg/kg **1** blood levels were assessed at increasing time points by mass spectrometry. As shown in Figure 11, the initial spike in concentration expected immediately following injection was observed. Surprisingly however, these levels rapidly decreased and returned to baseline by 60 min despite the fact that the PD analgesic response remained near maximal for at least 180 min. One possible explanation for the discrepancy between the PK and PD is that a hydrolysis product or an unidentified metabolite of **1** passes through the BBB to activate the NTRs and maintain the sustained analgesia well after **1** is degraded. To test this possibility, the kinetics of NTR-1 binding in the plasma of rats after injection of **1** were examined and are overlaid on the data in Figure 11. As shown, very quickly (1 min) after i.v. injection there is a large increase in NTR-1 binding which begins to rapidly decrease by 15 minutes. After 60 minutes, levels have returned to concentrations not significantly different from non-treated animals. Notably, the kinetic profile of receptor binding mirrored almost exactly the level of parental compound measured by mass spectrometry. Indeed, calculated half-lives (T_{1/2}) were 0.407 h and 0.438 h, respectively.

To further insure that metabolites of **1** were not responsible for the demonstrated PD response, the various possible hydrolytic metabolites of this compound were synthesized and the 5-mers and 4-mers assayed in the hotplate model. Table 2 lists these possible metabolites while Figure 12 shows the results of that analysis. In response to treatment with **1** response latency rapidly increased to maximum (30 s) and remained high during the course of the experiment. In contrast, no increase in response latency was seen with any of the possible metabolites. There was an early increase with **4** that did not approach maximal and rapidly returned to baseline; this is probably a spurious result. Because removal of one or two amino acids from either end completely abolished activity, further analysis of the 3 and 2-mers was deemed unnecessary. These results strongly argue that hydrolytic metabolites are not responsible for the long lasting PD effect observed with the parental compound.

Discussion

Neurotensin (NT) has been shown to be an effective endogenous pain modulator 27, and as such is an excellent candidate for pharmaceutical applications. However this peptide, and its fully active fragment NT(8–13), suffer from several druggability issues including deliverability, stability, selectivity and efficacy. When designing derivatives to address these issues, several elements of the peptide must be retained in order not to adversely degrade its activity. In particular, the positively charged side-chains at the N-terminus 2–8 and the free carboxylate at position 13 and are necessary for significant activity. Loss of potency also is noted when Arg⁸ is changed from L- to D- 28–29.

We have previously developed a derivative of NT(8–13), **2**, that retained the structural features necessary for activity but included a modified N-terminus and Arg⁸ residue, and substituted *t*Leu for Ile¹². This compound had strong anti-psychotic but weak analgesic activity. In this study a series of 43 additional analogs were synthesized that feature further modification of the N-terminus and Arg residue (Table 1). As anticipated, this resulted in compounds with a wide variety of activities in the hot plate model of acute pain.

A few generalizations can be made on the structure-function relationships of the current series of NT(8–13) derivatives. In the Arg⁸ position, nearly all Orn substituted derivatives (ABS209-ABS212 (**1**) and ABS234-ABS236) possessed significantly increased activity (five of eight analogs reached 100% MPE while two others were over 80%). The effect of the Orn substitution has been similarly reported for a class of NT(8–13)-based antipsychotic drugs **20**. In addition, analogs containing Arg⁸ plus a methyl addition (ABS214 and ABS238), or hLys alone (**2** and ABS225) performed quite well. In these cases activity was not affected by a change in the N-terminus group. These results indicate that smaller side chains at Arg⁸ are more effective analgesics. Overall, however, it was surprising that broader structure-activity relationships did not result from the data, which may indicate a complex cross-talk between binding and activating NTR-1 and NTR-2 to promote the observed physiological responses.

Data from the hotplate model enabled identification of **1** as the best lead candidate for further characterization. This molecule demonstrated a potent antinociceptive response in four additional rat analgesic models. The EC₅₀ values for three of the four i.v. analgesic tests were quite similar (approximately 2.0 mg/kg), validating the use of the hotplate model as an initial screening tool. A significantly lower EC₅₀ was detected in the acetic acid writhing assay which may be a result of the enhanced sensitivity of this assay relative to the others ^{23–24}.

This EC₅₀ did not differ due to route of administration suggesting it is freely permeable throughout the periphery. Repeated administration of **1** for 12 straight days did not result in the development of significant tolerance to the drugs even though previous studies with other NT(8–13) analogs found tolerance after a single dose ¹⁶.

Analysis of the PK of this drug surprisingly revealed that it is rapidly cleared from the circulation (<60 min), despite the fact that the analgesic response is maintained for nearly 4 hours. This possibly explains the absence of tolerance which is generally due to desensitization following long term exposure of drugs. The observed dichotomy between the PK and PD cannot be explained by a previously unrecognized metabolite of the analog because NTR-1 binding decreased at an identical rate to levels of parental compound measured by LC/MS. Moreover, none of the possible 5-mer or 4-mer hydrolytic metabolites of **1** possessed significant endogenous activity. Thus, the mechanisms of this PK/PD dichotomy remain undefined although it could be explained by selective uptake and distribution between the blood and the brain and/or compound binding to the central NTRs manifesting long-lived molecular changes that sustain the analgesic activity.

The discovery and development of peptide drugs provides the most direct route for exploiting genomic and proteomic insights into the treatment of disease. Peptides can act as agonists to positively affect biological processes, with the potential to repair damaged, injured, or undeveloped tissue. Peptide therapeutics represent an extremely powerful approach that can reduce the time and risk of bringing a drug to market. Compared to synthetic small molecules, drugs based on native peptides have the potential for shorter and more reliable development cycles because their physiological activity is well defined prior to development and they are much less likely to cause unexpected toxicities. We conclude

that **1** is an exciting new candidate for potential development as a broad-spectrum, first-in class, analgesic.

Experimental Section

Peptide Synthesis

Appropriately protected non-natural amino acid analogues of Arg and Lys were synthesized as described previously by our laboratory 30–35 and others 36 for incorporation at the 8 position of NT(8–13) via Merrifield solid-phase synthesis (Figure 1). All analogues were determined to be greater than 95% enantiomerically pure. Peptides were prepared by manual solid-phase peptide synthesis on Wang resin (Fmoc chemistry), purified by reverse-phase HPLC, and isolated and studied as the trifluoroacetate salts **19**. Peptide identity was determined by MALDI-TOFMS on a Voyager DE-STR System 4117 mass spectrometer (Applied Biosystems, Foster City, CA) and determined to be greater than 95% pure (MS data provided in Table 1).

Animals

All animal work was reviewed and approved by the Institutional Animal Care and Use Committee (IACUC) at the Medical University of South Carolina. Animal work at the University of California and Covance were reviewed and approved by their institutions' IACUCs. All experimental protocols were performed in accordance with the guidelines set forth in the NIH Guide for the Care and Use of Laboratory Animals, published by the Public Health Service. All protocols were performed on male Sprague-Dawley rats (Harlan, Prattville AL, 240–280g), which were housed in an AAALAC-approved colony room maintained at a constant temperature and humidity. Animals (two per cage) were kept on a 12-h light:dark cycle with ad libitum access to food and water. Because many of the assays are susceptible to learning phenomena, which results in progressive decrease of the physiological response or behavior to be monitored, rats were used no more than three times per analgesic assay. Only experimentally naïve rats were used in the formalin test.

Pain Models

Hotplate model—The hotplate model evaluates central pain attenuation in a rodent using an acute thermal stimulus known to be mediated through central processing pathways 37–39. In this assay the rat is treated with compound and, at a series of time points thereafter, assessed on a hotplate analgesia meter (Columbus Instruments, Columbus, OH), essentially a flat surface maintained at 53.0±0.2°C. After placing the rat on the hot surface the time until the rat lifts, nibbles or shakes one of its hind paws is recorded, which is known as the response latency. To avoid tissue damage, animals were not allowed to remain on the hotplate longer than 30 sec. The individual experiments were scored as the percent of maximal possible effect (%MPE) calculated using the following equation: %MPE = [(post-drug latency – pre-drug latency)/(cut-off pre-drug latency)] × 100%. The dose-response curves and ED₅₀ values were generated using GraphPad Prism®.

Acetic acid writhing model—This protocol is a well-established model of analgesia 40–42. Rats are administered drug i.v., and then rested for 20 min before i.p. injection with 2 ml/kg of 3% acetic acid. Animals were then placed in a 10 inch by 10 inch chamber and allowed to rest an additional 10 min. For the next 20 min, rats are observed every 20 sec. At each point individual rats are scored on whether they are writhing or not. Writhing is defined as a constriction of the abdominal area, often with extension of the hind legs. At the end of the observation period the percent of the time the animal was observed to be writhing was calculated. The dose-response curves and ED₅₀ values were generated using GraphPad Prism®.

Tail flick model—This model evaluates phasic pain, involving less surface area stimulation than the hotplate model 43. This protocol was performed by placing rats in individual Plexiglas containment and immersing the distal 3 cm of the rat's tail in a hot (49 +/- 1°C) water bath. The elapsed time was measured from insertion in the water to tail withdrawal. The cutoff latency for tail withdrawal was 10 s, at which time the animal's tail was removed from the water bath. Assays were scored as percent MPEs over time as discussed above (hotplate model). The dose-response curves and ED₅₀ values were generated using GraphPad Prism®.

Formalin model—The formalin model was performed according to the methods of Dubuisson and Dennis 44. As opposed to the procedures described above, this evaluates behavioral changes rather than changes in response latency and is considered a model of chronic pain. The rats were administered either control or test compound. Thirty minutes later, 50 µl of a 5% formalin solution in sterile saline was injected intradermally into the right forepaw. The animal was placed in a clear Plexiglas cage and the animal's posture was graded at one-minute intervals on a scale from 0–3 (0=normal posture, 1=paw on ground but not supporting rat, 2=paw raised, and 3=paw being licked, nibbled or shaken) for a period of 30 minutes (60 min post drug application). An average pain response was calculated for a minimum of 6 animals and plotted over time. The dose-response curves and ED₅₀ values were generated using GraphPad Prism®.

Chung model—The Chung model for neuropathic pain was performed in the laboratories of Tony Yaksh (University of California San Diego). To assess tactile thresholds, rats are placed in a clear plastic, wire mesh-bottomed cage, divided into individual compartments. Animals are allowed to acclimate and then baseline thresholds are assessed prior to drug treatment. To assess the 50% mechanical threshold for paw withdrawal, von Frey hairs are applied to the plantar mid-hind paw, avoiding the tori (footpads). The eight von Frey hairs used are designated by [log (10 * force required to bend hair, mg)] and range from 0.4–15.1 grams (#'s 3.61--5.18). Each hair is pressed perpendicularly against the paw with sufficient force to cause slight bending, and held for approximately 6–8 seconds. A positive response is noted if the paw is sharply withdrawn. Flinching immediately upon removal of the hair is also considered a positive response. Absence of a response ("-") is cause to present the next consecutive stronger stimulus; a positive response ("+") is cause to present the next weaker stimulus. Stimuli are presented successively until either six data points are collected, or the maximum or minimum stimulus is reached. If a minimum stimulus is reached and positive responses still occurred, the threshold is assigned an arbitrary minimum value of 0.25 grams; if a maximum stimulus is presented and no response occurred, a maximum threshold value of 15 grams is assigned. If a change in response occurs, either "-" to "+" or "+" to "-", causing a change in the direction of stimulus presentation from descending to ascending or vice-versa, four additional data points are collected subsequent to the change. The resulting pattern of responses are tabulated and the 50% response threshold computed using the formula

$$\log(\text{threshold, mg} \times 10) = Xf + kr;$$

where:

Xf = value of the last von Frey hair applied;

k = correction factor based on pattern of responses (from calibration table)

r = mean distance in log units between stimuli.

Based on observations on normal, un-operated rats and sham-operated rats, the cutoff of a 15.1-g hair is selected as the upper limit for testing 45.

Hypothermia Assay—Hypothermia assays were performed as previously described 46. Briefly, rats were placed in Plas-Labs[®] plastic restraining apparatuses (250–500 g model) and rectal probes (Physitemp[®], RET-2) lubricated with mineral oil and inserted in the animals' rectums. Probes were connected to a microprobe thermometer (Physitemp[®], BAT-12) equipped with a switchbox (Physitemp[®], SWT-5). Rats were allowed to equilibrate in the restraining apparatus for 15 min before initial temperatures were recorded. For injections, peptides were dissolved in saline and injected into the tail vein. Subsequent temperature measurements were taken every 15 min for 4 h. The area under the curve, the resulting dose-response curve and the EC₅₀ values were generated using GraphPad Prism[®] software.

Tolerance to the hot plate model—For tolerance experiments, six rats were separated into two groups of three. Both groups were injected i.v. with 10 mg/kg of **1** per day for 12 days consecutively. To avoid learning behaviors, each set was allowed at least 48 h between consecutive evaluations in the hotplate model as described above. Thus, any given data point represents the mean ±SEM of 3 rats (one set), although overall a total of 6 rats were analyzed for the development of tolerance.

NTR-1 and NTR-2 Binding Assays

Binding to rat NTR-1—NTR binding assays were performed as previously described 19. LTK cells expressing rat NTR were propagated in using standard cell culture techniques. For the assay, cells were scraped off the plates, washed and resuspended in binding buffer (20 mM Hepes (pH 7.4), 50 mM NaCl, 1.5 mM CaCl₂, 0.1 mg/ml L-lysine, 1% BSA, 0.01% NaN₃) at a concentration of 2×10^6 cells/ml. Samples for the determination of K_Ds were prepared by resuspending compound in binding buffer at various concentrations. For PK analysis, animals were sacrificed by CO₂ asphyxiation at the appropriate times and blood harvested into a pre-chilled heparin-coated tube by heart puncture. Tubes were then centrifuged (500 × g) to pellet cells and the resulting plasma was immediately aliquoted and frozen at -70 C for subsequent analysis. For generation of a standard curve, compound was resuspended and diluted in plasma isolated from untreated rats.

To perform the assay, 50 μl of sample was combined in a 1.5 ml microcentrifuge tube with 50 μl of cells (100,000 cells) and 50 μl containing 0.0375 pmol ¹²⁵I]-NT (approximately 100,000 CPM; diluted in binding buffer). The mixture was allowed to incubate 60 min at room temperature to come to equilibrium. Following incubation, 1 ml of ice cold binding buffer was added, the cells pelleted and the supernatants aspirated. Cells were washed again in 1 ml ice cold binding buffer and the tip of the tubes containing the pelleted cells cut off and counted in a gamma counter.

Binding to human NTR-1 and NTR-2—These studies were performed essentially as described previously 19. Briefly, cells transfected with either the hNTR-1 or hNTR-2 plasmids were homogenized and prepared as previously described 47. 10–50 μg of membranes were incubated for 20 min (25 °C) in 250 μl binding buffer (50 mM Tris-HCl, pH 7.5, containing 0.1% bovine serum albumin) with 0.4 nM ¹²⁵I-Tyr(3)-NT (2000 Ci/mmol) and various concentrations of unlabeled **1**. After incubation solutions were filtered through cellulose acetate filters and the filters rinsed twice with 3 ml ice cold binding buffer and counted in a Packard γ-counter. Nonspecific binding was determined in the presence of 1 μM unlabeled NT and represented less than 5% of the total binding.

Calcium Release Assay—NTR-1 is a G-protein coupled receptor that associates with Gq/11 to stimulate calcium release from the ER. This release was measured using a Calcium No Wash Plus Assay Kit from DiscoverX Inc. (Fremont, CA). LTK cells expressing NTR1 were plated at 20,000 cells/well in 100 μ l in a 96-well black, clear bottom plate and incubated overnight. Media was then removed by inverting the plate and then 100 μ l/well of dye reagent was added (prepared as recommended by the manufacturer). Plates were then incubated 1 h at 37°C before being analyzed for calcium release in response to various concentrations of compound (prepared in binding buffer) using a Fluorometric Imaging Plate Reader (FLIPR; Molecular Devices Corporation) that automatically injects various doses of compound prepared in the binding buffer used above (20 mM Hepes (pH 7.4), 50 mM NaCl, 1.5 mM CaCl₂, 0.1 mg/ml L-lysine, 1% BSA, 0.01% NaN₃). Maximal response was determined by treatment with 1 μ M of ionomycin whereas background was determined by treatment with binding buffer alone. Responses were calculated as the percent of the maximal response after subtraction of background. EC₅₀ values were determined using GraphPad Prism[®] software.

PK analysis by Liquid Chromatography/mass spectrometry (LC/MS)—PK analysis by LC/MS/MS was performed by Covance laboratories Inc. (Madison, WI). Briefly, rats were injected i.v. via the tail vein with 1 mg/kg **1**, then blood samples (approximately 0.75 mL) were collected from 2 or 3 animals per time point from a jugular vein via syringe and needle and transferred into tubes containing sodium heparin anticoagulant maintained on wet ice. Samples were centrifuged and plasma placed into 96-well plates, quick frozen on dry ice and stored at -70°C until used. Samples were then extracted and subjected to HPLC/MS analysis using Covance proprietary methods. The maximum concentration (C_{max}) in plasma and the time to reach maximum concentration (T_{max}) were obtained by visual inspection of the raw data. PK parameters calculated included half-life (t_{1/2}), area under the concentration-time curve from time 0 to the last time point (AUC_{0-t}), and area under the concentration-time curve from 0 to infinity (AUC_{0-∞}). PK parameters were calculated by using WinNonlin Professional Edition (Pharsight Corporation, Version 5.2).

Abbreviations

NT	neurotensin
BBB	blood brain barrier
NTS	neurotensin receptor
CNS	central nervous system
MPE	maximum possible effect
PK	pharmacokinetic
PD	pharmacodynamic

Acknowledgments

The authors wish to thank Dr. Tony Yaksh and colleagues at the University of California at San Diego for performing the Chung assay. This work was supported by Grant # GM-079044 (T.A.D., P.I.) from the National Institutes of Health, National Institute of General Medical Sciences. This research was conducted in a facility constructed with support from the National Institutes of Health, Grant Number C06 RR015455 from the Extramural Research Facilities Program of the National Center for Research Resources.

References

1. Carraway R, Leeman SE. The isolation of a new hypotensive peptide, neurotensin, from bovine hypothalami. *J. Biol. Chem.* 1973; 248:6854–6861. [PubMed: 4745447]
2. Carraway, R.; Leeman, S. Structural requirements for the biological activity of neurotensin, a new vasoactive-peptide. In: Walter, R.; Meienhofer, J., editors. *Peptides: Chemistry, Structure and Biology*. Ann Arbor: Ann Arbor Science; 1975. p. 679-685.
3. Rioux FKR, Quirion R, St-Pierre S. Mechanisms of the cardiovascular effects of neurotensin. *Ann. N.Y. Acad. Sci.* 1982; 400:56–74. [PubMed: 6963116]
4. Rosell S, Rokaesus A. Actions and possible hormonal functions of circulating neurotensin. *Clin. Physiol.* 1981; 1:3–20.
5. Nemeroff CB, Osbahr AJ, Manberg PJ, Ervin GN, Prange AJ. Alterations in nociception and body temperature after intracisternal administration of neurotensin, β -endorphin, other endogenous peptides, and morphine. *Pro. Nat. Acad. Sci.* 1979; 76:5368–5371.
6. Bissette G, Nemeroff C, Loosen P, AJ Prange J, Lipton M. Hypothermia and intolerance to cold induced by intracisternal administration of the hypothalamic peptide neurotensin. *Nature Biotech.* 1976; 262:607–609.
7. Nemeroff CB. Neurotensin: perchance an endogenous neuroleptic? *Biol. Psychiatry.* 1980; 15:283–302. [PubMed: 6106513]
8. Skoog KM, Cain ST, Nemeroff CB. Centrally administered neurotensin suppresses locomotor hyperactivity induced by d-amphetamine but not by scopolamine or caffeine. *Neuropharmacol.* 1986; 25:777–782.
9. Pettibone DJ, Hess JF, Hey PJ, Jacobson MA, Leviten M, Lis EV, Mallorga PJ, Pascarella DM, Snyder MA, Williams JB, Zeng Z. The effects of deleting the mouse neurotensin receptor NTR1 on central and peripheral responses to neurotensin. *J. Pharmacol. Exp. Ther.* 2002; 300:305–313. [PubMed: 11752130]
10. Remaury A, Vita N, Gendreau S, Jung M, Arnone M, Poncelet M, Culouscou JM, Le Fur G, Soubrie P, Caput D, Shire D, Kopf M, Ferrara P. Targeted inactivation of the neurotensin type 1 receptor reveals its role in body temperature control and feeding behavior but not in analgesia. *Brain Res.* 2002; 953:63–72. [PubMed: 12384239]
11. Kokko KP, Arrigoni CE, Dix TA. Selectivity enhancement induced by substitution of non-natural analogues of arginine and lysine in arginine-based thrombin inhibitors. *Bioorg. Med. Chem. Lett.* 2001; 11:1947–1950. [PubMed: 11459667]
12. Tyler BM, Cusack B, Douglas CL, Souder T, Richelson E. Evidence for additional neurotensin receptor subtypes: neurotensin analogs that distinguish between neurotensin-mediated hypothermia and antinociception. *Brain Res.* 1998; 792:246–252. [PubMed: 9593920]
13. Hadden MK, Orwig KS, Kokko KP, Mazella J, Dix TA. Design, synthesis, and evaluation of the antipsychotic potential of orally bioavailable neurotensin (8–13) analogues containing non-natural arginine and lysine residues. *Neuropharmacol.* 2005; 49:1149–1159.
14. Machida R, Tokumura T, Tsuchiya Y, Sasaki A, Abe K. Pharmacokinetics of novel hexapeptides with neurotensin activity in rats. *Biol. Pharm. Bull.* 1993; 16:43–47. [PubMed: 8369751]
15. Tyler-McMahon BM, Stewart JA, Farinas F, McCormick DJ, Richelson E. Highly potent neurotensin analog that causes hypothermia and antinociception. *Eur. J. Pharmacol.* 2000; 390:107–111. [PubMed: 10708713]
16. Boules M, McMahon B, Wang R, Warrington L, Stewart J, Yerbury S, Fauq A, McCormick D, Richelson E. Selective tolerance to the hypothermic and anticataleptic effects of a neurotensin analog that crosses the blood-brain barrier. *Brain Res.* 2003; 987:39–48. [PubMed: 14499944]
17. Cusack B, McCormick DJ, Pang YP, Souder T, Garcia R, Fauq A, Richelson E. Pharmacological and biochemical profiles of unique neurotensin 8–13 analogs exhibiting species selectivity, stereoselectivity, and superagonism. *J. Biol. Chem.* 1995; 270:18359–18366. [PubMed: 7629159]
18. Dubuc I, Sarret P, Labbe-Jullie C, Botto J-M, Honore E, Bourdel E, Martinez J, Costentin J, Vincent J-P, Kitabgi P, Mazella J. Identification of the receptor subtype involved in the analgesic effect of neurotensin. *J. Neurosci.* 1999; 19:503–510. [PubMed: 9870978]

19. Kokko KP, Hadden MK, Orwig KS, Mazella J, Dix TA. In vitro analysis of stable, receptor-selective neurotensin[8–13] analogues. *J. Med. Chem.* 2003; 46:4141–4148. [PubMed: 12954066]
20. Hadden MK, Walle T, Dix TA. Cellular uptake of a radiolabelled analogue of neurotensin in the Caco-2 cell model. *J. Pharmacy & Pharmacol.* 2005; 57:327–333.
21. Orwig KS, Lassetter MR, Hadden MK, Dix TA. Comparison of N-terminal modifications on neurotensin(8–13) analogues correlates peptide stability but not binding affinity with in vivo efficacy. *J Med Chem.* 2009; 52:1803–1813. [PubMed: 19290594]
22. Clineschmidt B, McGuffin J. Neurotensin administered intracisternally inhibits responsiveness of mice to noxious stimuli. *Eur. J. Pharmacol.* 1977; 46:395–396. [PubMed: 201475]
23. Coquerel A, Dubuc I, Kitaegi P, Costentin J. Potentiation by thiorphan and bestatin of the naloxone-insensitive analgesic effects of neurotensin and neuromedin n. *Neurochem. Int.* 1988; 12:361–366. [PubMed: 20501239]
24. Costentin J, Vlaiculescu A, Chaillet P, Ben Natan L, Aveaux D, Schwartz JC. Dissociated effects of inhibitors of enkephalin-metabolising peptidases or naloxone on various nociceptive responses. *Eur J Pharmacol.* 1986; 123:37–44. [PubMed: 3519246]
25. Myers RM, Shearman JW, Kitching MO, Ramos-Montoya A, Neal DE, Ley SV. Cancer, chemistry, and the cell: molecules that interact with the neurotensin receptors. *ACS Chem Biol.* 2009; 4:503–525. [PubMed: 19462983]
26. Cusack B, Jansen K, McCormick DJ, Chou T, Pang Y, Richelson E. A single amino acid of the human and rat neurotensin receptors (subtype 1) determining the pharmacological profile of a species-selective neurotensin agonist. *Biochemical Pharmacology.* 2000; 60:793–801. [PubMed: 10930533]
27. Dobner P. Neurotensin and pain modulation. *Peptides.* 2006; 27:2405–2414. [PubMed: 16870306]
28. Henry JA, Horwell DC, Meecham KG, Rees DC. A structure-affinity study of the amino acid side-chains in neurotensin : N and C terminal deletions and Ala-scan. *Bioorg. & Med. Chem. Lett.* 1993; 3:949–952.
29. Kitabgi P, Poustis C, Granier C, Van Rietschoten J, Rivier J, Morgat J-L, Freychet P. Neurotensin binding to extraneural and neural receptors: comparison with biological activity and structure--activity relationships. *Mol. Pharmacol.* 1980; 18:11–19. [PubMed: 6251356]
30. Hadden MK, Kokko KP, Dix TA. Asymmetric synthesis of ω -bromo-2(S)-methyl acids as precursors for novel aginine, lysine, and mercapto reidues. *Synthetic Comm.* 2005; 35:1675–1680.
31. Kennedy KJ, Lundquist IVJT, Simandan TL, Beeson CC, Dix TA. Asymmetric synthesis of non-natural homologues of lysine. *Bioorg. & Med. Chem. Lett.* 1997; 7:1937–1940.
32. Kennedy KJS, T.L, Dix TA. A facile route to cyclic and acyclic alkyl-arginines. *Syn. Comm.* 1998; 28:741–746.
33. Kennedy KJ, Lundquist JTt, Simandan TL, Kokko KP, Beeson CC, Dix TA. Design rationale, synthesis, and characterization of non-natural analogs of the cationic amino acids arginine and lysine. *J. Pep. Res.* 2000; 55:348–358.
34. Kokko KP, Brooks Hooper H, Dix TA. Synthesis of cyclic and acyclic N[α]-methyl-N[ω]-alkyl--arginine analogues. *Tetrahedron Lett.* 2004; 45:2151–2153.
35. Lundquist JTI, Orwig KS, Dix TA. Synthesis of ethylene-bridged (N δ to N ω) analogues of arginine. *J. Org. Chem.* 1999; 64:9265–9267.
36. Lundquist, JTt; Pelletier, JC. Improved solid-phase peptide synthesis method utilizing alpha-azide-protected amino acids. *Org. Lett.* 2001; 3:781–783. [PubMed: 11259061]
37. Marchioro M, Blank Mde F, Mourao RH, Antonioli AR. Anti-nociceptive activity of the aqueous extract of *Erythrina velutina* leaves. *Fitoterapia.* 2005; 76:637–642. [PubMed: 16242270]
38. Ridditid W, Sae-Wong C, Reanmongkol W, Wongnawa M. Antinociceptive activity of the methanolic extract of *Kaempferia galanga* Linn in experimental animals. *J Ethnopharmacol.* 2008; 118:225–230. [PubMed: 18486374]
39. Wong CH, Dey P, Yarmush J, Wu W-H, Zbuzek VK. Nifedipine-induced analgesia after epidural injection in rats. *Anesthesia and Analgesia.* 1994; 79:303–306. [PubMed: 7639369]
40. Barber A, Bartoszyk GD, Bender HM, Gottschlich R, Greiner HE, Harting J, Mauler F, Minck KO, Murray RD, Simon M, et al. A pharmacological profile of the novel, peripherally-selective kappa-opioid receptor agonist, EMD 61753. *Br J Pharmacol.* 1994; 113:1317–1327. [PubMed: 7889287]

41. Barber A, Gottschlich R. Opioid agonists and antagonists: an evaluation of their peripheral actions in inflammation. *Med Res Rev.* 1992; 12:525–562. [PubMed: 1513187]
42. Vanderah TW, Scheingart CD, Trojnar J, Junien JL, Lai J, Riviere PJ. FE200041 (D-Phe-D-Phe-D-Nle-D-Arg-NH₂): A peripheral efficacious kappa opioid agonist with unprecedented selectivity. *J Pharmacol Exp Ther.* 2004; 310:326–333. [PubMed: 14993260]
43. Grotto M, Sulman F. Modified receptacle method for animal analgesimetry. *Arch. Int. Pharmacodyn. Ther.* 1967; 165:152–159. [PubMed: 5339935]
44. Dubuisson D, Dennis S. The formalin test: a quantitative study of the analgesic effects of morphine, meperidine and brain stem stimulation in rats and cats. *Pain.* 1977; 4:161–174. [PubMed: 564014]
45. Chaplan SR, Bach FW, Pogrel JW, Chung JM, Yaksh TL. Quantitative assessment of tactile allodynia in the rat paw. *J. Neurosci. Methods.* 1994; 53:55–63. [PubMed: 7990513]
46. Kokko KP, Hadden MK, Price KL, Orwig KS, See RE, Dix TA. In vivo behavioral effects of stable, receptor-selective neurotensin[8–13] analogues that cross the blood-brain barrier. *Neuropharmacol.* 2005; 48:417–425.
47. Chabry J, Labbe-Jullie C, Gully D, Kitabgi P, Vincent JP, Mazella J. Stable expression of the cloned rat brain neurotensin receptor into fibroblasts: binding properties, photoaffinity labeling, transduction mechanisms, and internalization. *J. Neurochem.* 1994; 63:19–27. [PubMed: 8207427]

ABS Neurotensin Library
R = Arg-Pro-Tyr-tLeu-Leu-OH

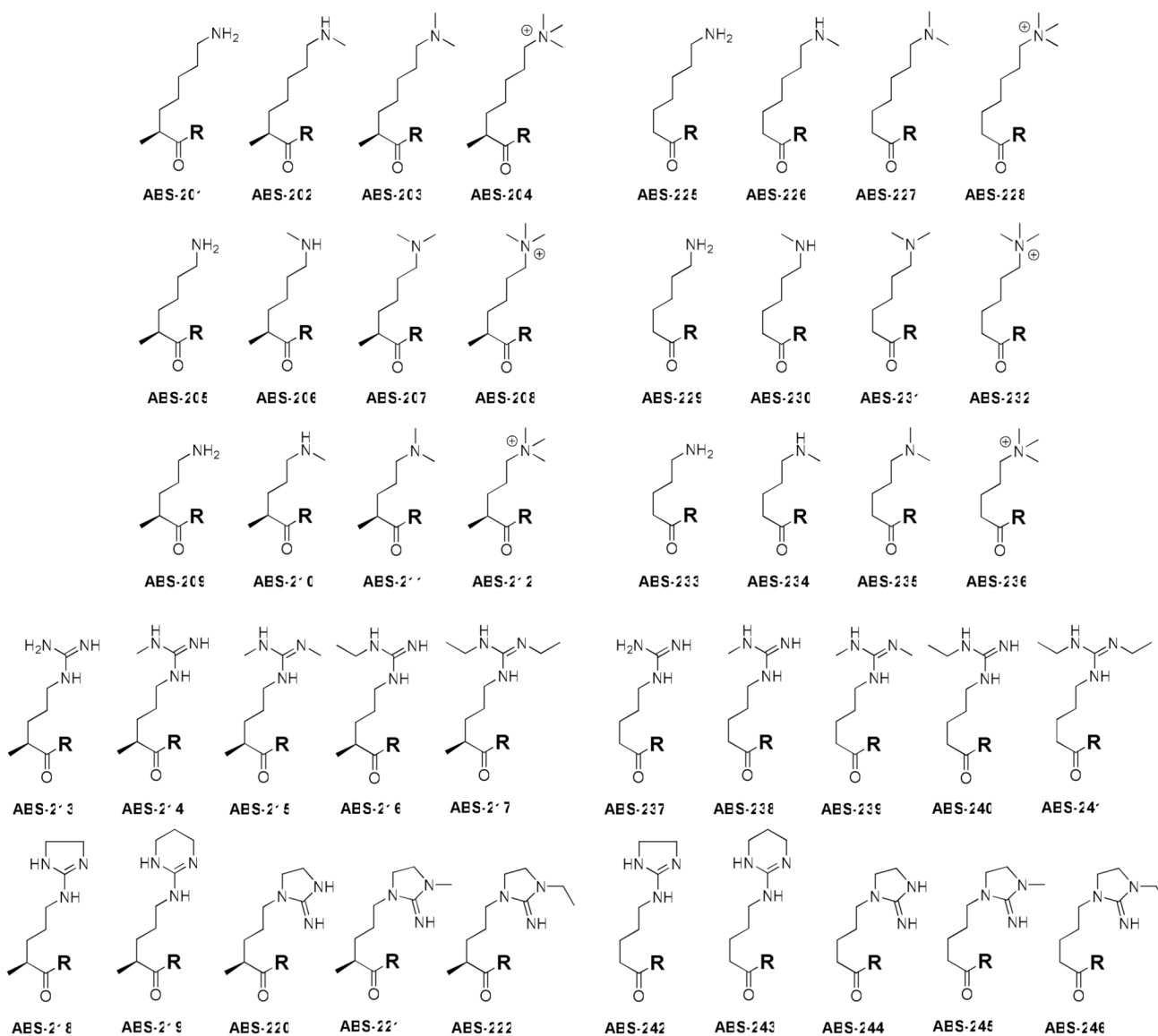


Figure 1. Structures of cationic natural and non-natural amino acids substituted for Arg 8 in NT(8–13)

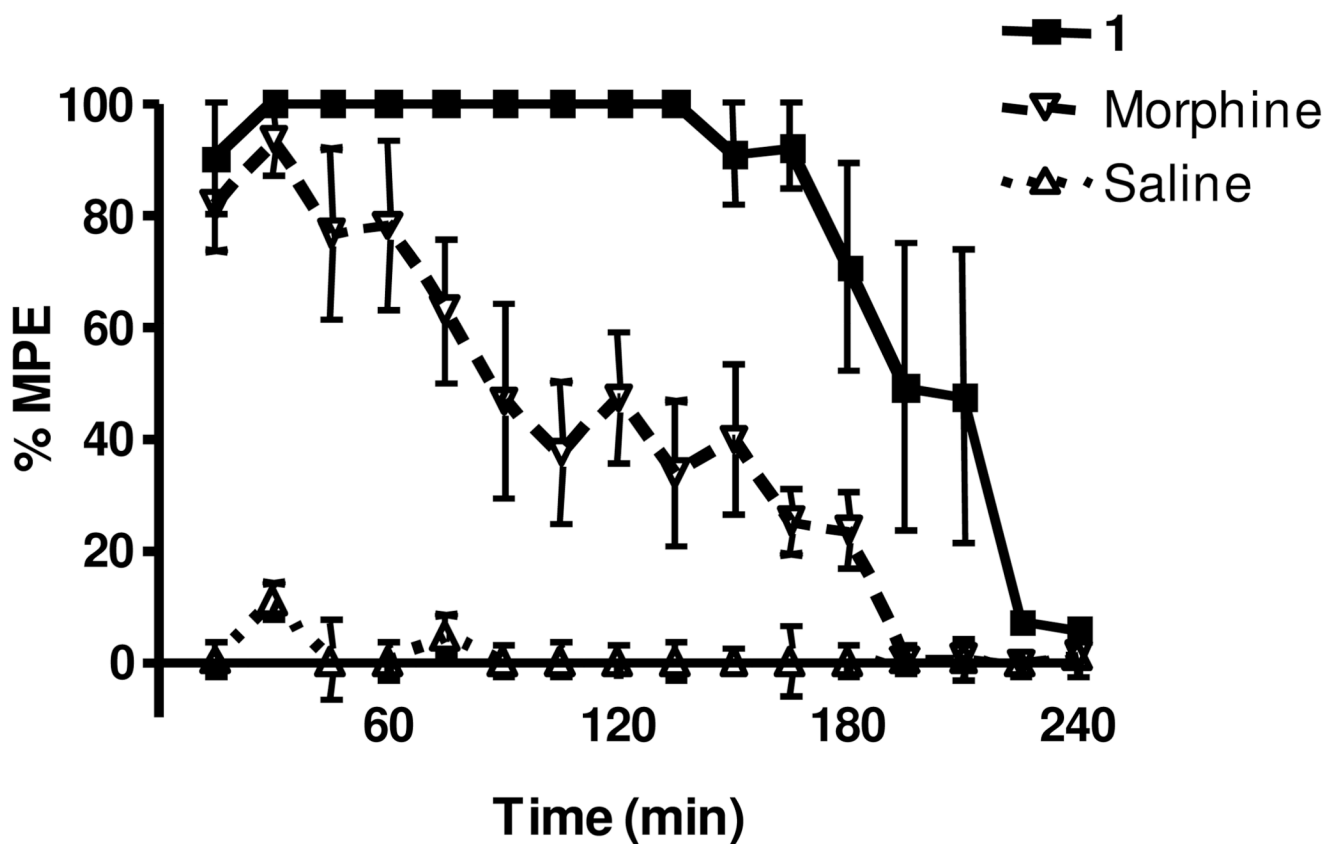


Figure 2. Compound **1** benchmarked with morphine in the hotplate model. Rats were dosed i.p. with either **1** at 10 mg/kg, morphine at 5 mg/kg, or sterile saline and analyzed at the indicated time points in the hotplate model. Individual points indicate the mean \pm SEM. $n \geq 6$ for all treatments.

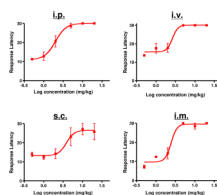


Figure 3.

Effect of route of administration of **1** in the hotplate model. Rats were injected either i.p., i.v., s.c. or i.m. with various concentrations of **1** and then assessed in the hotplate assay after 60 min. EC₅₀s were: i.p. = 2.00 mg/kg (95% confidence levels of 1.543 and 2.583); mg/kg, i.v. = 2.64 mg/kg (95% confidence levels of 1.261 and 5.546 mg/kg); s.c. = 3.84 mg/kg (95% confidence levels of 1.567 and 9.392 mg/kg; i.m. 2.45 mg/kg (95% confidence levels of 1.376 and 4.369 mg/kg). n = 3 for all doses. Individual points indicate the mean \pm SEM.

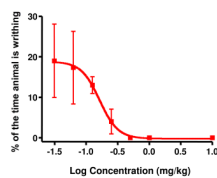


Figure 4. Dose-response of **1** in the writhing model. Rats received varying concentrations of **1** i.v. before analysis in the writhing model. $EC_{50} = 0.16$ mg/kg, with 95% confidence levels of 0.07269 and 0.3669 mg/kg, $n = 3$ for all doses. Individual points indicate the mean \pm SEM.

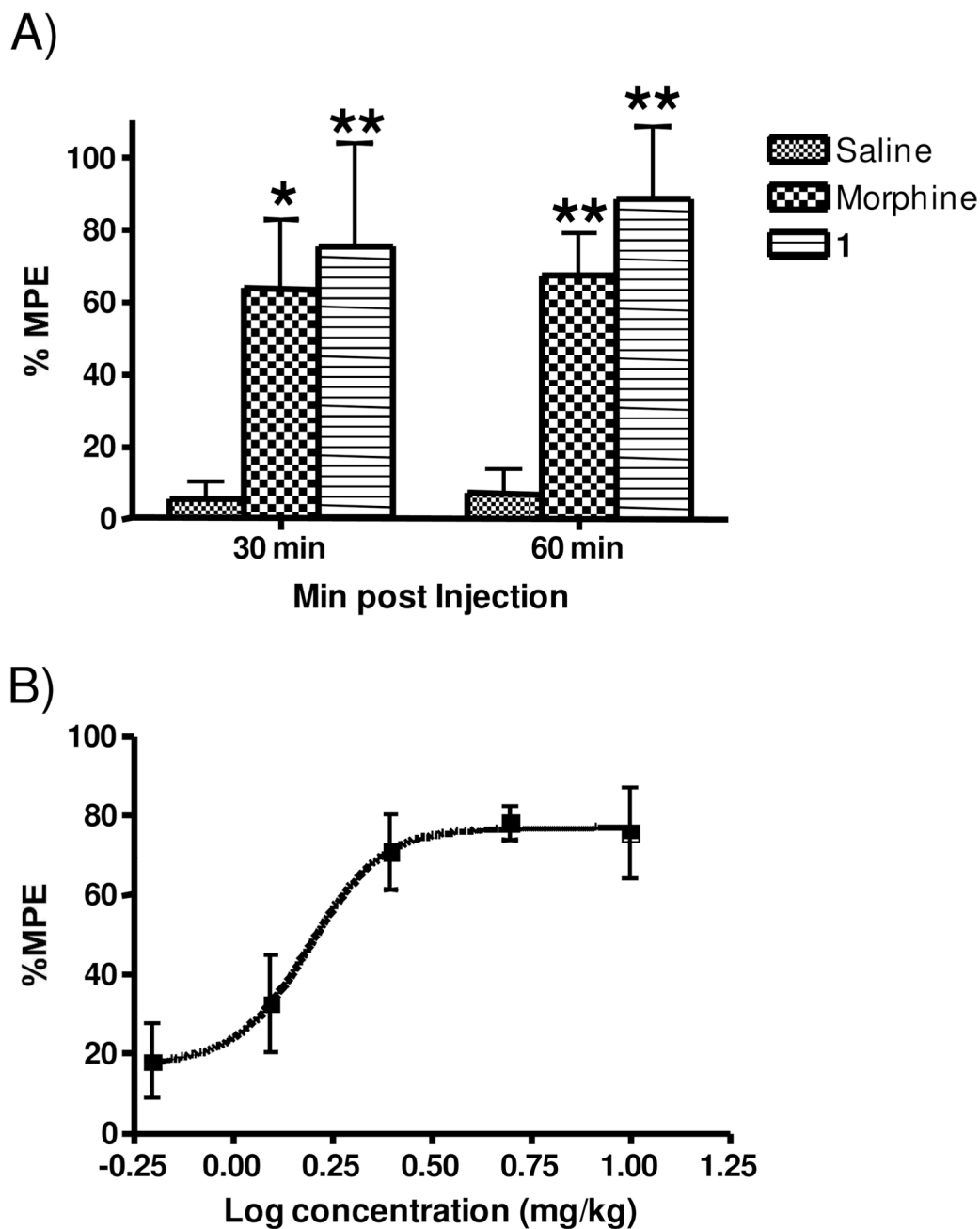


Figure 5. Effects of **1** in the tail flick model. **A.** Typical PD response elicited by **1**, morphine and saline. Rats were dosed i.p. with either **1** at 10 mg/kg, morphine at 5 mg/kg, or sterile saline and analyzed in the tail flick assay at 30 min and 60 min, $n = 6$ for each treatment. Individual points indicate the mean \pm SEM. Single asterisks denote values significantly different from saline with a p value < 0.05 whereas double asterisks indicate $p < 0.01$. **B.** Dose response of **1**. Rats were injected i.p. with various doses of **1** and assessed in the tail flick model 30 min later. The EC_{50} was 1.57 mg/kg, with 95% confidence levels of 0.967 and 2.552 mg/kg, $n = 6$ for all doses. Individual points indicate the mean \pm SEM.

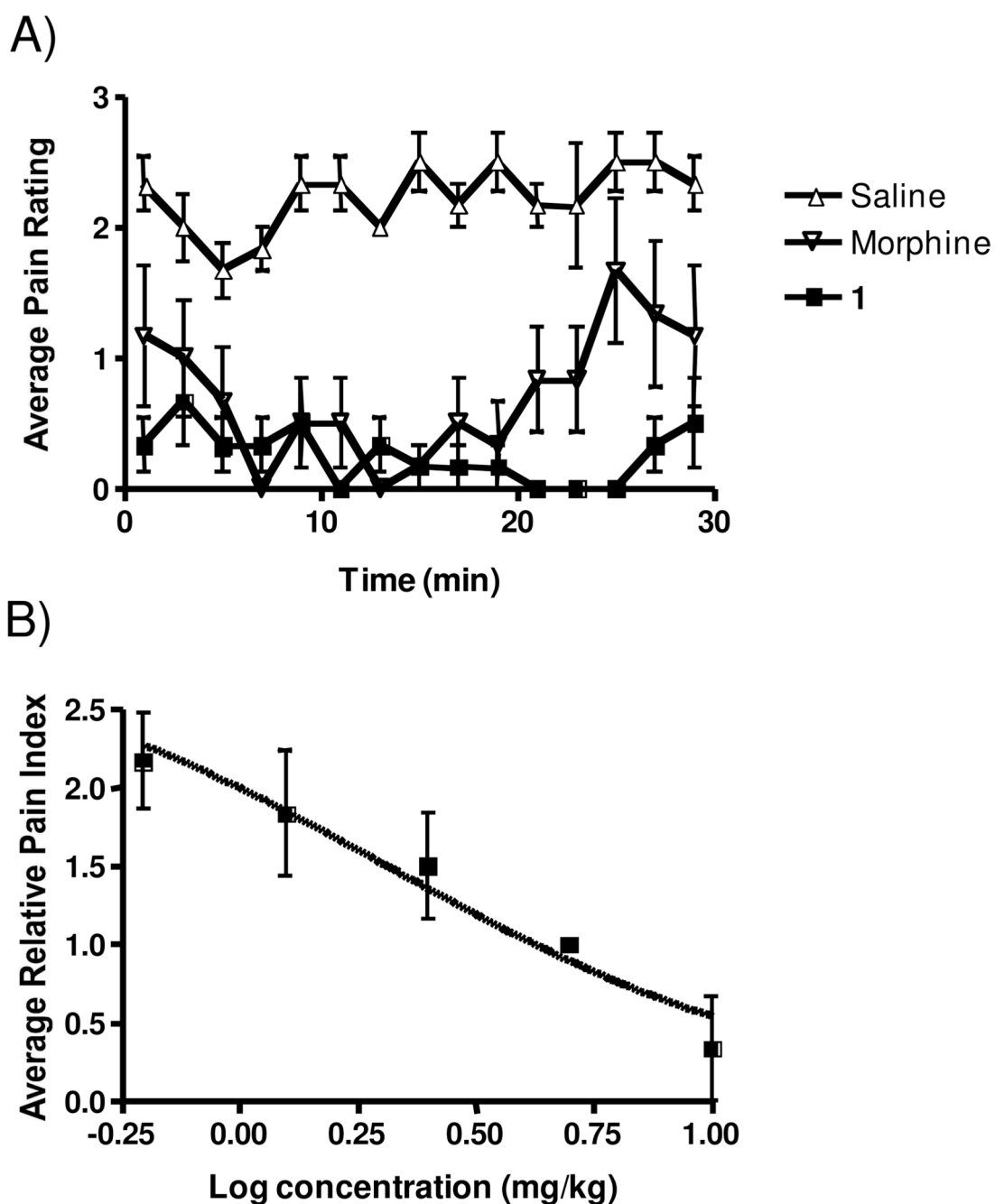


Figure 6. Effect of **1** in the formalin model. **A.** Typical PD response elicited by **1**, morphine and saline. Rats were dosed i.p. with either **1** at 10 mg/kg, morphine at 5 mg/kg, or sterile saline and analyzed in the formalin assay for 30 min, $n = 6$ for each treatment. Individual points indicate the mean \pm SEM. **B.** Dose response of **1**. Rats were injected i.p. with various doses of **1** and assessed in the tail flick model 30 min later. The EC_{50} was 2.06 mg/kg, with 95% confidence levels of 1.27 and 3.30 mg/kg. $n = 6$ for all doses. Individual points indicate the mean \pm SEM.

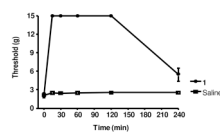


Figure 7. Effect of **1** in the Chung model. Rats were given an i.p. dose of either 10 mg/kg **1** or saline and analyzed in the Chung assay for 30 min, $n = 5$ for both treatments. Individual points indicate the mean \pm SEM.

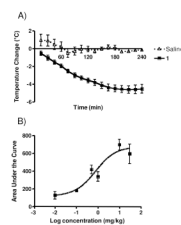


Figure 8.

Effect of **1** in the hypothermia assay. **A.** Typical PD response elicited by **1** and saline. Rats were dosed i.v. with either **1** at 10 mg/kg or sterile saline and analyzed in the hypothermia assay for 4 h, $n \geq 4$ for each treatment. Individual points indicate the mean \pm SEM. **B.** Dose response of **1**. Rats were injected i.v. with various doses of **1** and assessed in the hypothermia assay. The total area under the various PD curves was calculated and used to generate the dose-response curve. $EC_{50} = 0.78$ mg/kg with 95% confidence levels of 0.190 and 3.237 mg/kg, $n = 3$ for all doses. Individual points indicate the mean \pm SEM.

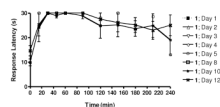


Figure 9.

Evaluation of tolerance development in response to repeated daily doses of **1**. Rats (6) were separated into two groups of three and both groups were injected i.v. with 10 mg/kg of **1** per day for 12 days consecutively. Each set was allowed at least 48 h between consecutive evaluation in the hotplate model. Thus, any given data point represents the mean \pm SEM of 3 rats (one set), although overall a total of 6 rats were analyzed for the development of tolerance.

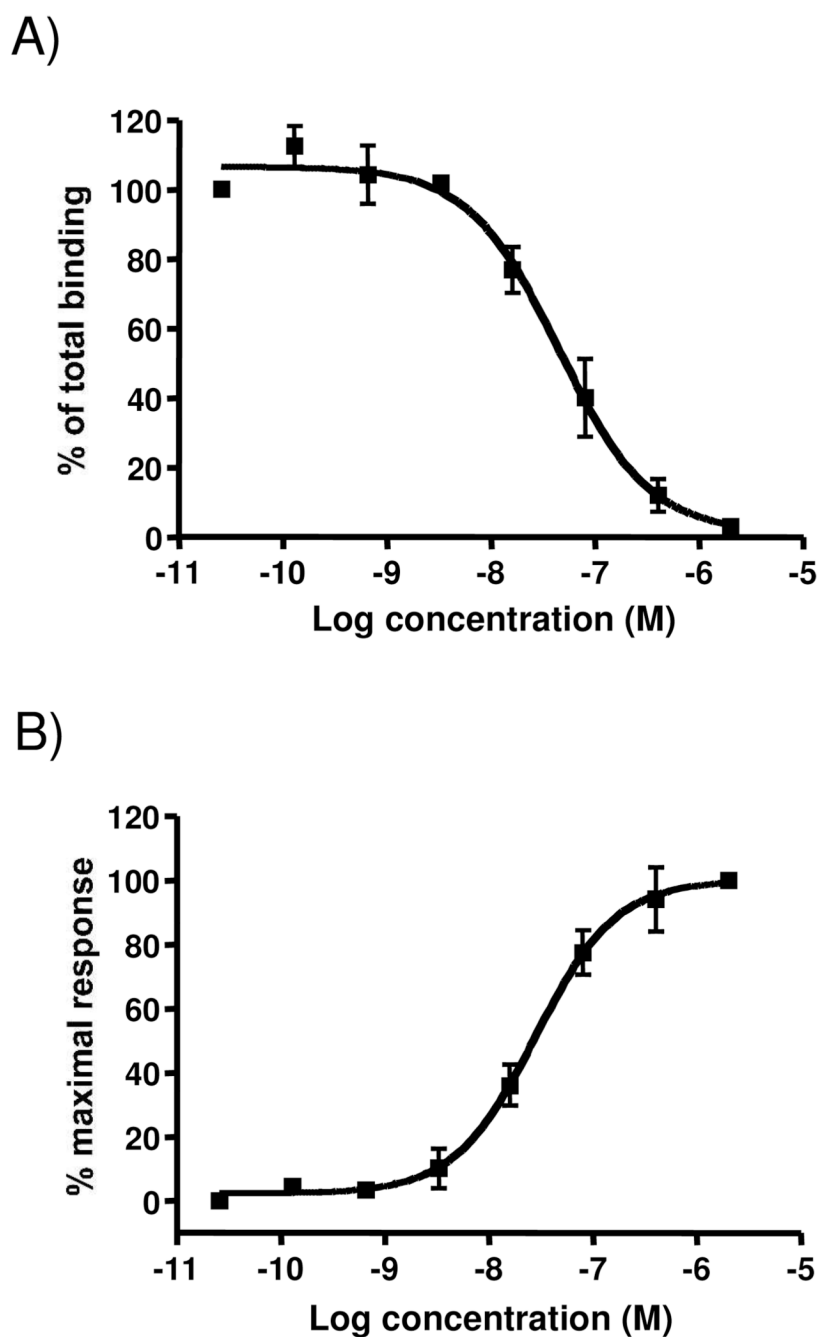


Figure 10.

Evaluation of **1** binding and activation of rat NTR-1. **A.** Radioligand competition assays with ^{125}I -NT were performed and the data normalized to percent of maximal binding. Individual experiments were measured in triplicate and each experiment was performed a minimal of 3 independent times. The data points represent the mean \pm SEM of all experiments. The K_i was 23.31 nM with 95% confidence levels of 14.01 and 38.79 nM. **B.** Calcium release assays were performed on the Fluorometric Imaging Plate Reader (FLIPR; Molecular Devices Corporation). Individual points indicate the mean \pm SEM of at least three independent measurements. The EC_{50} was 27.88 nM with 95% confidence levels of 17.62 and 44.10nM.

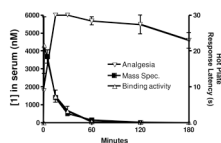


Figure 11.

PK analysis of **1** levels and receptor binding activity overlaid on PD information from the hot plate model. Rats were injected with 1 mg/kg **1**. At each time point of 1 (or 5), 15, 30, 60, 120, 180 and 240 min, 3 rats were assessed using the hot plate model. Thus, individual points represent the mean \pm SEM of three independently assessed rats. Animals were immediately sacrificed after analysis and plasma isolated and analyzed in the NTR-1 radiolabel competition assay. Thus, individual points represent the mean \pm SEM of three independently assessed rats. Plasma concentrations were calculated from a standard curve prepared in plasma from untreated rats. Plasma levels of **1** were also assessed by MS in a separate experiment performed by Covance, Inc. Individual points represent the mean \pm SEM of at least three independently assessed rats.

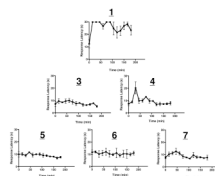


Figure 12.

Evaluation of all potential 5- and 4-mer hydrolysis products of **1** in the hot plate model. All possible 5 and 4-mer products that might result from proteolysis from the N-terminal, the C-terminal, or both were synthesized and injected into rats i.v. at 12.5 mmols/kg. The change in concentration from mg/kg was necessary to insure equimolar levels given the differences in molecular weights. Each graph is the individual PD response curve for that hydrolysis product and each point on the graphs represents the mean \pm SEM of at least three rats independently assessed at that time point.

Table 1

Comparison of peptides in the Hot Plate Assay. Three major endpoints are compared; 1) the maximal possible effect (MPE) that was obtained with that drug, 2) the time that the maximal effect was maintained and 3) the area underneath the pharmacodynamic response curve.

Compound	m/e (obs/calc)	MPE	Time at MPE (m)	AUC
201 (2)	802.60/802.02	100.00	45	9928
202	816.63/816.04	100.00	75	12182
203	830.65/830.07	60.94	0	4281
204	844.72/845.10	19.90	0	1898
205	788.60/787.99	86.00	0	11015
206	802.64/802.02	55.80	0	6001
207	816.65/816.04	84.90	0	7004
208	830.68/831.08	67.20	15	8788
209	774.60/773.96	89.40	0	9507
210	788.60/787.99	82.40	0	12105
211	nd	nd	nd	nd
212 (1)	816.59/817.05	100.00	135	18084
213	816.56/816.00	48.52	0	3515
214	830.60/830.03	100.00	75	8874
215	844.69/844.06	63.30	0	6106
216	844.63/844.06	74.48	0	12400
217	872.72/872.11	10.00	0	781
218	842.65/842.04	79.31	0	5793
219	nd	nd	nd	nd
220	nd	55.00	0	3569
221	856.71/856.07	76.07	0	7462
222	nd	nd	nd	nd
225	788.67/787.99	100.00	*60	8416
226	802.65/802.02	59.32	0	5345
227	816.75/816.04	29.00	0	3985
228	830.79/831.08	55.70	0	3853
229	774.61/773.96	48.00	0	3520
230	788.64/787.99	100.00	30	5733
231	nd	nd	nd	nd
232	816.69/817.05	84.00	0	11109
233	760.62/759.94	51.69	0	3585
234	774.33/773.96	100.00	120	17320
235	788.40/787.99	100.00	90	11180
236	802.42/803.02	100.00	60	7022
237	802.44/801.98	50.86	0	4039

Compound	m/e (obs/calc)	MPE	Time at MPE (m)	AUC
238	816.48/816.00	100.00	75	8396
239	830.51/830.03	92.28	0	5152
240	830.55/830.03	37.36	0	2148
241	858.68/858.08	95.68	15	7425
242	828.57/828.01	76.40	0	7506
243	842.63/842.04	79.62	0	6637
244	828.69/828.01	82.80	0	6110
245	nd	nd	nd	nd
246	856.69/856.07	80.48	0	7119

Table 2

The 5-mer and 4-mer hydrolytic fragments of **1**.

cpd	length	structure			m/e (obs/calc)
3	5-mers	Me3-Orn	Arg	Pro Tyr tLeu	703.52/704.88
4			Arg	Pro Tyr tLeu Leu	661.47/660.80
5	4-mers	Me3-Orn	Arg	Pro Tyr	590.38/5912.70
6			Arg	Pro Tyr tLeu	548.30/547.61
7				Pro Tyr tLeu Leu	nd